Available online at www.sciencedirect.com
ScienceDirect
Catalysis Today 116 (2006) 439–444
CATALYSIS TODAY
www.elsevier.com/locate/cattod

# Kinetic study of the redox process for storing hydrogen Reduction stage

J.A. Peña *, E. Lorente, E. Romero, J. Herguido

*Catalysis, Molecular Separations and Reactor Engineering Group (CREG), Aragón Institute for Engineering Research ($I^3A$), University of Zaragoza, 50018 Zaragoza, Spain*

Available online 7 July 2006

**Abstract**

The redox process, the reduction of metal oxides and subsequent oxidation by steam to release hydrogen, is an interesting alternative to other methods of storing hydrogen. In order to evaluate the suitability of different metallic oxides for this purpose, either alone ($Fe_2O_3$) or as mixed oxides ($NiFe_2O_4$, $CuFe_2O_4$), a kinetic study has been carried out by means of a thermogravimetric system.

The kinetic parameters of the reduction of the oxides by hydrogen have been calculated by fitting experimental data with suitable "ad hoc" models for non-catalytic gas–solid reactions. The addition of a second metal to form double oxides has a positive effect, since these exhibit greater reaction rates.



*Keywords:* Hydrogen storage; Redox process; Iron oxides; Kinetic study; Hydrogen purification

## 1. Introduction

Widespread use of hydrogen as an energy carrier could address growing concerns about energy supply, global climate change and air quality. Hydrogen offers the long-term potential of an energy system that produces near-zero emissions and can be derived from a variety of primary sources (including fossil fuels and renewable sources). Despite these benefits, an economic exploitation of hydrogen poses multiple challenges. Although hydrogen production, storage and delivery technologies are currently in commercial use by the chemical and refining industries, existing hydrogen storage and conversion technologies are still not competitive for expanded use in energy applications. Therefore, much fundamental research, into areas including production, storage, delivery, and end-use applications remains to be done [1,2].

One of the major obstacles to the use of hydrogen as an energy carrier is the lack of safe, efficient, and low cost storage systems, suitable for stationary and mobile applications. Various methods are currently being proposed and developed for its direct or indirect storage [3]. Hydrogen can be stored as a discrete gas or liquid (physical storage) or in a chemical compound (chemical storage). Compressed gas storage is at present the most long-standing and commercially dominant technology available, although it is subject to the problem of relatively low energy densities which leads to inefficient use of space for transportation and onboard applications [4]. Liquid hydrogen takes up less storage volume than gas but requires cryogenic containers. Furthermore, the liquefaction of hydrogen is an energy-intensive process and results in large evaporative losses (almost half of the lower heating value of hydrogen is lost in the process [5]). A number of other technologies, including metal hydride, hydrogen absorbing alloys and carbon nanotubes, are under development for storage; however, these are still constrained by weight to volume limits [6,7]. Although each storage method has desirable attributes, no current approach appears to satisfy all the desired efficiency, size, weight, cost, and safety requirements for transportation or utility use.

As a promising alternative for the storage and supply of pure hydrogen, the redox process, that is, the reduction of metal oxides and subsequent oxidation by steam to release

* Corresponding author. Fax: +34 976 761879.
*E-mail address:* jap@unizar.es (J.A. Peña).

0920-5861/$ – see front matter © 2006 Elsevier B.V. All rights reserved.
doi:10.1016/j.cattod.2006.05.068

hydrogen, has recently been proposed [8,9]. The technology is based on a simple redox reaction of a metal oxide (Eqs. (1) and (2)):

$$M_xO_y + yH_2 \rightarrow xM + yH_2O \quad (1)$$

$$xM + yH_2O \rightarrow M_xO_y + yH_2 \quad (2)$$

The process operates in two stages: during the first step the metal oxide (denoted as $M_xO_y$) is reduced by a gas stream containing hydrogen into the metal. Water is also produced and is eliminated by condensation outside of the reactor. In the second step, and subsequently, the metal is oxidized with water vapour into the oxide to form hydrogen. This is a simple, safe, and environmentally benign method, in which hydrogen is ''chemically stored'' as a reduced metal. The most commonly used metal oxide mediators for the storage of hydrogen are iron oxides ($Fe_2O_3$, $Fe_3O_4$), due to their high redox capacity, availability and economic feasibility [10–14].

The principle of the redox technology is analogous to the old *steam iron process* developed in the late 19th/early 20th century to produce hydrogen rich fuel gas at high temperatures and pressures for the reduction of iron ores [15] by using gas mixtures of CO, $CO_2$ and $H_2$ from gasified coal. This two-step process can also be used as a way to selectively separate hydrogen from other gases, such as hydrogen-containing natural gas and those resulting from natural gas reforming, hydrocarbon (including natural gas) and biomass pyrolysis or gasification [16–19].

This paper describes the results of a kinetic study carried out to gain insight into the reduction step of the redox process, obtain data for the selection and design of a suitable reactor and establish the optimal reaction conditions for such a purpose. Several candidate oxides, either alone ($Fe_2O_3$) or as mixed oxides ($NiFe_2O_4$, $CuFe_2O_4$), were used in order to evaluate their suitability for the process.

## 2. Experimental

### 2.1. Materials preparation

Samples of three oxides ($Fe_2O_3$, $NiFe_2O_4$, $CuFe_2O_4$) were prepared as bulk oxides by the citrate method [20]. The samples were synthesized from $Fe(NO_3)_3{\cdot}9H_2O$ (98.0%, Panreac), $Ni(NO_3)_2{\cdot}6H_2O$ (98.0%, Aldrich) and $Cu(NO_3)_2{\cdot}2.5H_2O$ (98.0%, Aldrich). The starting metal salts were dissolved in distilled water to the desired concentration (1 M). For mixed oxides, the amounts of metal nitrates were fitted to form a mixture with an equimolar relation ratio between both cations. An aqueous solution of citric acid (99.0%, Aldrich) was then added to the solution of metal nitrates, with a citric acid to salt ratio of 1:1. During the addition, the solution was maintained in a stirred glass vessel at 80 °C. The gel formed was dried overnight in an oven at 110 °C. The material was subsequently calcined at 800 °C in air for 6 h.

### 2.2. Characterization techniques

The prepared oxides were characterised by different methods.

Phase characterization was carried out by X-ray diffraction (XRD), using Cu Kα radiation (λ = 1.5418 Å). The data were collected in the $2\theta$ range from 15° to 80° in 0.03° steps.

The Brunauer–Emmett–Teller (BET) surface area was determined by $N_2$ adsorption at 77 K, using the Micromeritics Pulse Chemisorb 2700 device.

Temperature programmed reduction (TPR) measurements were conducted in order to obtain the characteristic temperatures of hydrogen consumption. A feed of 5% $H_2$ in $N_2$ at a flow rate of 100 mL $min^{-1}$ (STP) was used as reducing gas. The samples (typically 200 mg) were heated up to 800 °C, at a rate of 5 °C $min^{-1}$. The hydrogen consumption was monitored using a thermal conductivity detector.

### 2.3. Activity tests and kinetic study

The reduction of the oxide samples was performed in a CI Electronics thermobalance.

Oxide samples of 20 mg, with a sieve fraction of 100–160 μm, atmospheric pressure and total flow rates of 750 mL $min^{-1}$ (STP) were used in all the experiments. Previous experiment series were conducted ranging sample mass, sieve size and flow rates in order to assure that no bed depth effect or diffusional limitations were present during the kinetic tests.

Dynamic experiments with hydrogen (diluted in $N_2$) were conducted by heating the samples at a rate of 5 °C $min^{-1}$ up to 800 °C. Similar experiments were carried out using $CH_4$ as reducing gas, in order to evaluate the ability of the studied oxides to separate $H_2/CH_4$ mixtures with the redox process.

In order to find the kinetic parameters for the reduction of the oxides with hydrogen, a set of isothermal experiments were carried out over the range of hydrogen partial pressure (diluted in $N_2$) from 0.1 to 0.9 atm and temperatures varying from 320 to 440 °C (with different temperature intervals for each oxide).

The degree of reduction of the sample (DR) was defined as the ratio of weight loss at any time to the total weight loss after complete reduction:

$$DR = \frac{\text{weight loss at time } t}{\text{weight loss after complete reduction}} \quad (3)$$

## 3. Results and discussion

### 3.1. Material properties

The X-ray diffractograms of the prepared $Fe_2O_3$ (Fig. 1), $NiFe_2O_4$ and $CuFe_2O_4$ (Fig. 2) confirmed the predicted structures of the oxides. The BET surface areas of the three oxides, $Fe_2O_3$, $NiFe_2O_4$ and $CuFe_2O_4$, were relatively small: 2.3, 6.5 and 0.4 $m^2/g$, respectively.

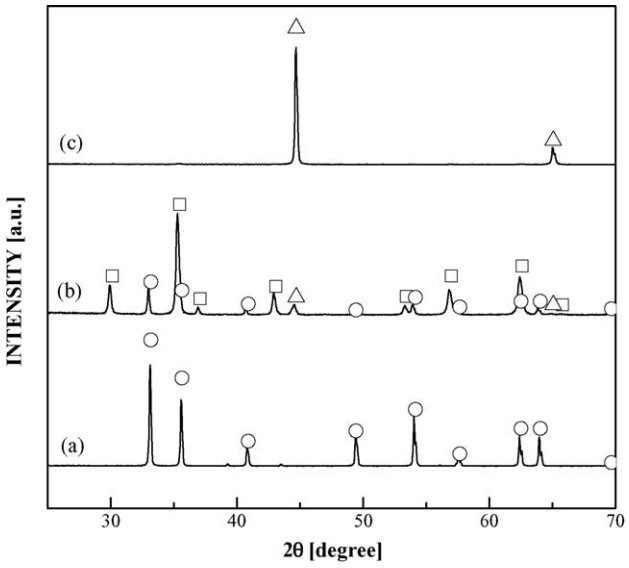


Fig. 1. XRD patterns of iron oxide: (a) before reaction, (b) after partial reduction, DR ≈ 11% and (c) after complete reduction. (○) Hematite; (□) magnetite; (△) metallic iron.

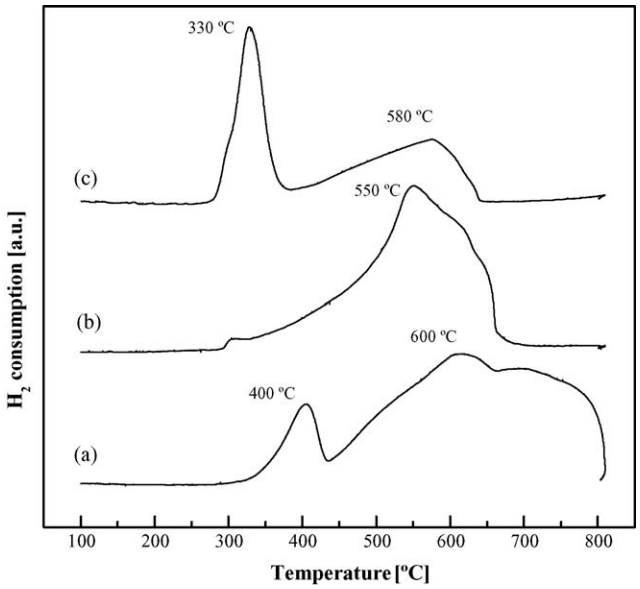


Fig. 3. TPR profiles of (a) $Fe_2O_3$, (b) $NiFe_2O_4$ and (c) $CuFe_2O_4$.

The TPR profiles of the three oxide materials are shown in Fig. 3. For $Fe_2O_3$, two peaks were observed at around 400 and 600 °C. The low-temperature peak can be attributed to the reduction of $Fe_2O_3$ to $Fe_3O_4$ while the high-temperature peak could be caused by the reduction of $Fe_3O_4$ to Fe. It is known that the addition to the hematite structure of certain metal ions, such as $Cu^{2+}$, $Ni^{2+}$, etc., as doping agents causes a decrease in the reduction temperature [21]. This is especially true for the $Cu^{2+}$ ion. The mixed oxides studied in the present work exhibit this behaviour, which leads to a decrease in the temperature of the first reduction peak (in the TPR profiles).

Fig. 4 shows the results of the dynamic experiments with hydrogen and methane, carried out in the thermobalance system, for each of the oxides studied, $Fe_2O_3$, $NiFe_2O_4$ and $CuFe_2O_4$. The hydrogen reduction curves confirm the higher reactivity of the mixed oxides (lower values of the initial reduction temperatures) compared to pure $Fe_2O_3$. Exposure of these metal oxides to $CH_4$ showed that the reduction of the oxides appears at high temperatures (almost 500 °C). At such temperatures, complete reduction of the oxides with hydrogen has been achieved. This result shows the advantage of selectively separating $H_2$ from $H_2/CH_4$ mixtures by means of the redox process.

### 3.2. Reduction behaviour of $Fe_2O_3$

Since $Fe_2O_3$ was taken as a basis, experiments of reduction with hydrogen (diluted in $N_2$) were carried out in order to check out its behaviour. Fig. 5A and B shows the degree of reduction versus time curves obtained with several hydrogen partial pressures and different temperatures, respectively.

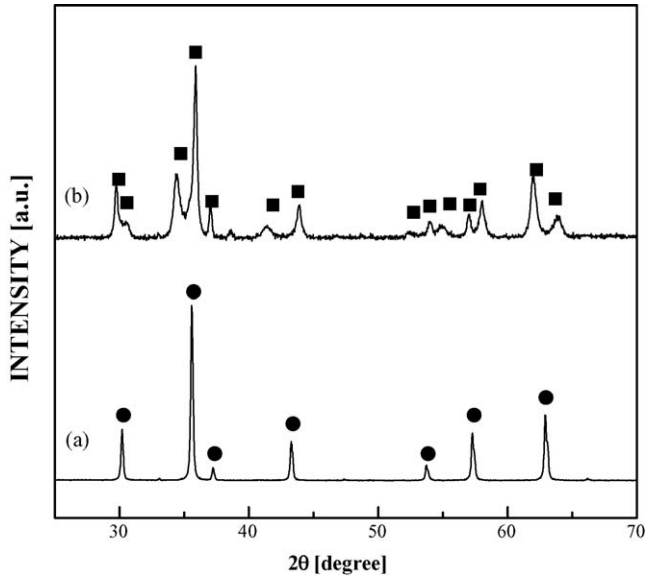


Fig. 2. XRD patterns of mixed iron oxides: (a) $NiFe_2O_4$ and (b) $CuFe_2O_4$. (●) $NiFe_2O_4$; (■) $CuFe_2O_4$.

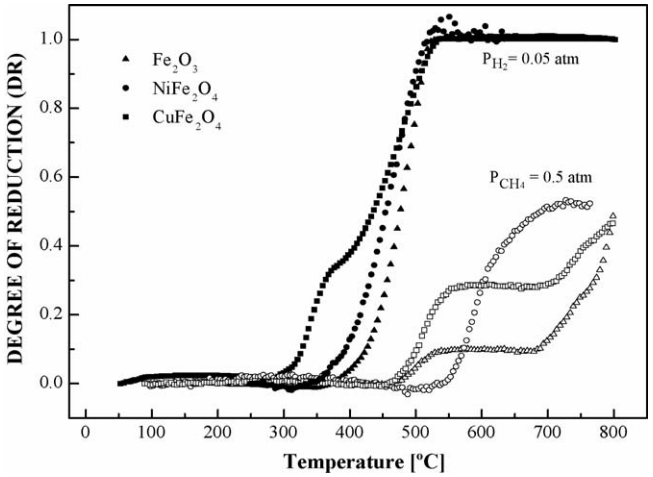


Fig. 4. Degree of reduction vs. temperature curves for $Fe_2O_3$, $NiFe_2O_4$ and $NiFe_2O_4$ reduction with hydrogen (solid) and methane (void).

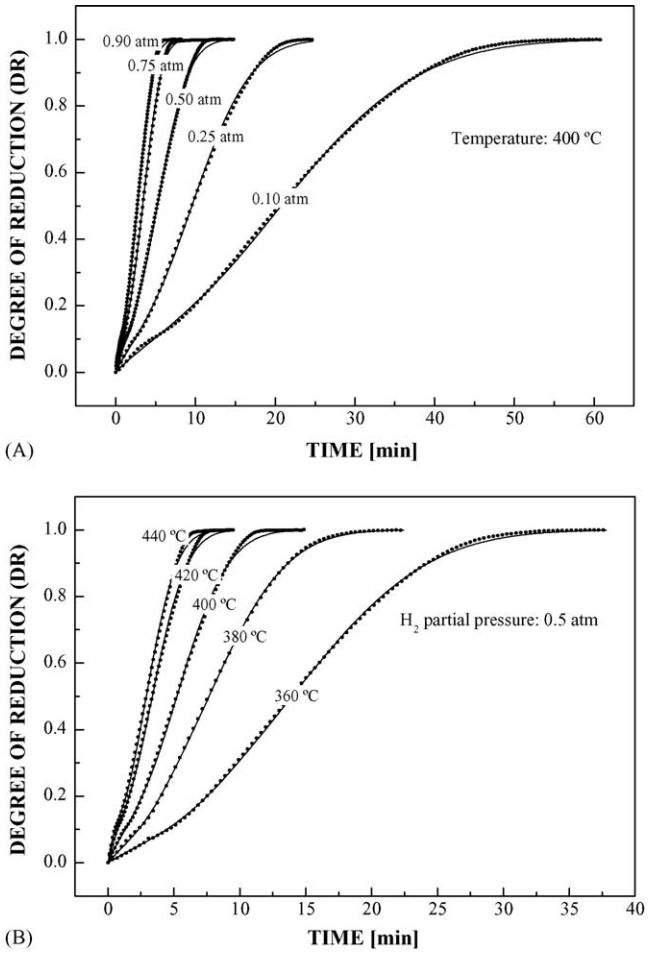


Fig. 5. Degree of reduction vs. time curves for $Fe_2O_3$ reduction with different hydrogen partial pressures (A) and different temperatures (B). Experimental (scatter) and fitted (solid line) data.

The typical shape of the curves (also reported elsewhere [14,21,22]), with a shoulder at a degree of reduction of about 10–12%, points to a stepwise reaction via $Fe_3O_4$ (that implies a stoichiometric DR of 11.1%), with overlapping of two reduction processes (Eqs. (4) and (5)):

$$\text{Step1}: \quad 3Fe_2O_3 + H_2 \rightarrow 2Fe_3O_4 + H_2O \tag{4}$$

$$\text{Step2}: \quad Fe_3O_4 + 4H_2 \rightarrow 3Fe + 4H_2O \tag{5}$$

To obtain further evidence about the intermediate oxides, X-ray diffraction studies were carried out on a completely and a partially reduced sample of about 11% degree of reduction. Fig. 1 shows the XRD patterns of fresh ($Fe_2O_3$) and processed samples. While the fresh and the completely reduced samples were formed exclusively by $Fe_2O_3$ (hematite) and iron, respectively, the partially reduced sample was mainly composed of $Fe_3O_4$ (magnetite) with small amounts of $Fe_2O_3$ and Fe.

In order to obtain more insight into the mechanism and the kinetic parameters describing the two-step $Fe_2O_3$ reduction, a model was investigated. Various models have appeared in the literature for interpreting kinetic data from gas–solid non-catalytic multistep reactions [23]. These models are based on the assumption that the same reaction mechanism is applied to all the steps. This interpretation is inconsistent with the degree of reduction–time curves observed for hematite reduction.

In order to describe such behaviour, a model has been proposed comprising the sum of two former models, with proper coefficients derived from the stoichiometry of the reaction. The first reduction step could be described with the *shrinking core model* (SCM) [23]. On the other hand; two different models previously used for interpreting the reduction of $Fe_3O_4$ with hydrogen (that is, the second step) were proposed: the *crackling core model* (CCM) [24,25] and the Avrami or *nucleation model* (AM) [26–29].

The joining of the *shrinking core* for the first step and the Avrami for the second (SCA model) proved to be the best model to fit the experimental data. The expression of DR as a function of time, as well as the relations of the characteristic parameters $\tau$ and $M$ with the operating temperature ($T$) and hydrogen concentration ($C$) are shown in Eqs. (6)–(8), respectively:

$$\text{DR} = \left(1 - \left(1 - \frac{t}{\tau}\right)^3\right)(0.11 + 0.89(1 - \exp(-Mt^N))) \tag{6}$$

$$\tau = \frac{1}{C^{n_1} k_1 \exp(-E_1/RT)} \tag{7}$$

$$M = C^{n_2} k_2 \exp\left(-\frac{E_2}{RT}\right) \tag{8}$$

where $t$ is the time (min), $\tau$ the characteristic parameter of the SCM, $M$ the characteristic parameter of the AM—global reaction rate constant, $N$ the characteristic parameter of the AM—nucleation exponent, $n_1$, $n_2$, the reaction order for step 1 (Eq. (4)) and step 2 (Eq. (5)), $k_1$, $k_2$, the pre-exponential factor for step 1 (Eq. (4)) and step 2 (Eq. (5)), $E_1$, $E_2$, are the activation energy for step 1 (Eq. (4)) and step 2 (Eq. (5)).

The values of the parameters $n_1$, $k_1$, $E_1$, $N$, $n_2$, $k_2$ and $E_2$ obtained by fitting the experimental data as well as the value of the model selection criterion (MSC) [30], are summarised in Table 1.

### 3.3. Reduction behaviour of mixed oxides: $NiFe_2O_4$ and $CuFe_2O_4$

The addition of NiO and CuO to the pure $Fe_2O_3$ was investigated in order to check the improvement of the redox properties versus the original iron oxide. The effect of

Table 1
Values of the characteristic parameters of the SCA model for the reduction of $Fe_2O_3$ with hydrogen

| | |
|---|---|
| $n_1$ | $0.82 \pm 0.16$ |
| $k_1$ ($m^3$/mol min) | $3.78 \times 10^7 \pm 0.12 \times 10^7$ |
| $E_1$ (kJ/mol) | $115.62 \pm 17.57$ |
| $N$ | $2.31 \pm 0.03$ |
| $n_2$ | $2.10 \pm 0.03$ |
| $k_2$ ($m^6$/mol$^2$ $min^2$) | $1.10 \times 10^{10} \pm 0.50 \times 10^{10}$ |
| $E_2$ (kJ/mol) | $179.52 \pm 3.06$ |
| MSC | 7.4 |

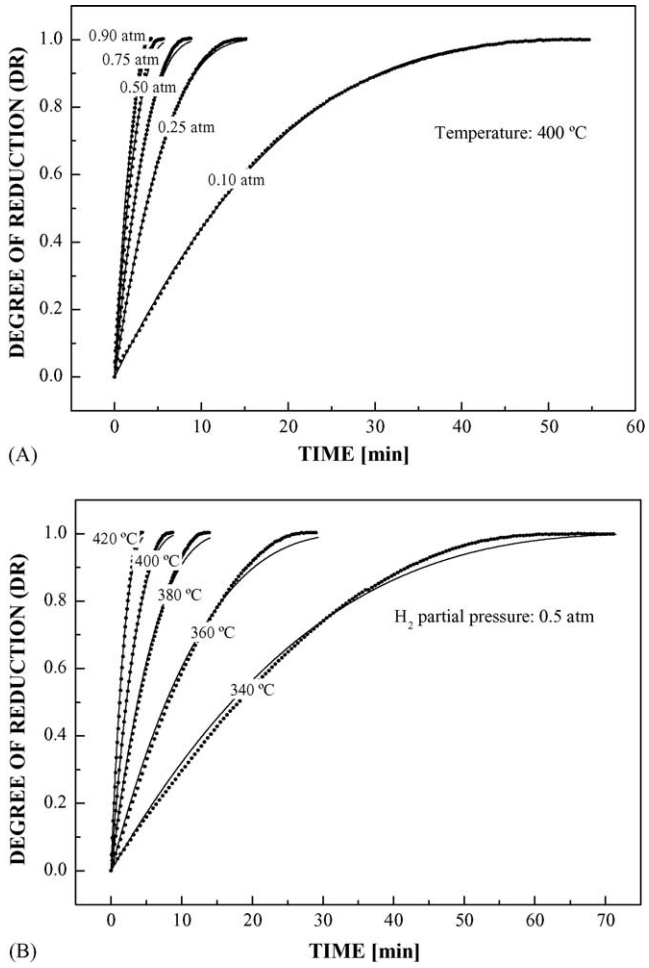


Fig. 6. Degree of reduction vs. time curves for $NiFe_2O_4$ reduction with different hydrogen partial pressures (A) and different temperatures (B). Experimental (scatter) and fitted (solid line) data.

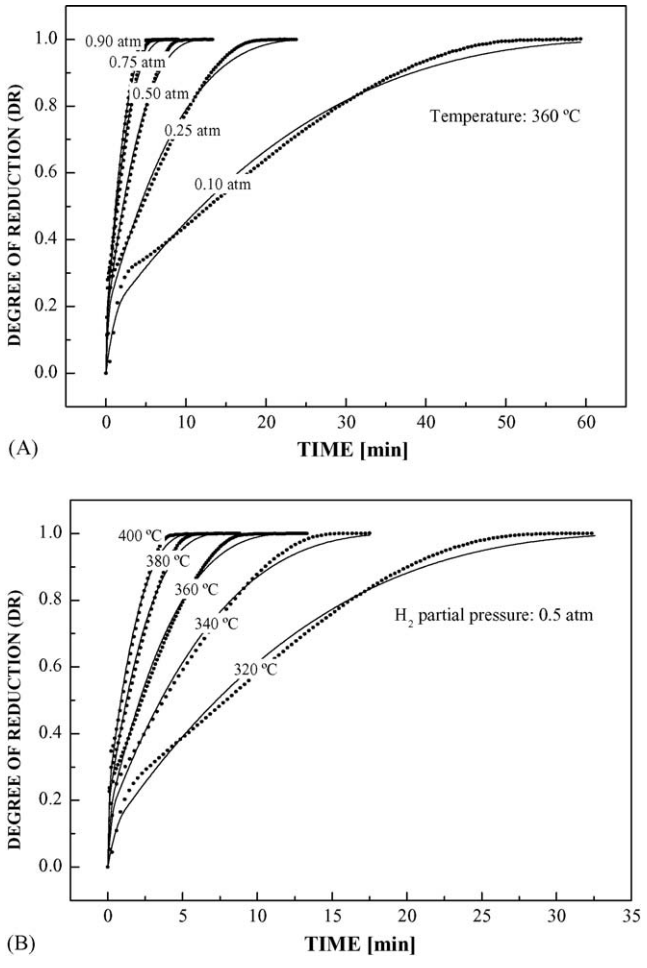


Fig. 7. Degree of reduction vs. time curves for $CuFe_2O_4$ reduction with different hydrogen partial pressures (A) and different temperatures (B). Experimental (scatter) and fitted (solid line) data.

temperature and hydrogen partial pressure on the reduction of the mixed oxides is shown in Fig. 6 ($NiFe_2O_4$) and Fig. 7 ($CuFe_2O_4$). The kinetic parameters of both reduction processes were also calculated.

Table 2
Values of the characteristic parameters of the shrinking core model for the reduction of $NiFe_2O_4$ with hydrogen

| | |
|---|---|
| $n$ | $1.00 \pm 0.005$ |
| $k$ ($m^3$/mol min) | $1.38 \times 10^7 \pm 0.11 \times 10^7$ |
| $E$ (kJ/mol) | $117.32 \pm 0.43$ |
| MSC | 5.6 |

Table 3
Values of the characteristic parameters of the crackling core model for the reduction of $CuFe_2O_4$ with hydrogen

| | |
|---|---|
| $n_c$ | $1.10 \pm 0.09$ |
| $k_c$ ($m^3$/mol min) | $1.94 \times 10^5 \pm 0.14 \times 10^5$ |
| $E_c$ (kJ/mol) | $73.11 \pm 13.72$ |
| $n_g$ | $1.10 \pm 0.006$ |
| $k_g$ ($m^3$/mol min) | $2.30 \times 10^4 \pm 0.92 \times 10^4$ |
| $E_g$ (kJ/mol) | $79.54 \pm 4.34$ |
| MSC | 5.1 |

Conversion degree versus time data for the reduction of $NiFe_2O_4$ were fitted to a *shrinking core model*, the simplest one-parameter ($\tau$) model for gas–solid non-catalytic reactions. Data for the reduction of $CuFe_2O_4$ was able to be properly fitted with the *crackling core model*: a model with two characteristic parameters, $\tau_c$ (time for complete disappearance of the virgin core) and $\tau_g$ (time for complete conversion of a grain). Taking into account the DR-time expressions of the models [23,24], and the relation of the parameters, $\tau$, $\tau_c$ and $\tau_g$ with the temperature ($T$) and hydrogen concentration ($C$) variables, shown in Eq. (9), the kinetic parameters $n_i$, $k_i$ and $E_i$ were obtained. The values of these parameters are summarised in Tables 2 and 3.

$$\tau_i = \frac{1}{C^{n_i} k_i \exp(-E_i/RT)}, \quad i = -, \mathrm{c}, \mathrm{g} \tag{9}$$

## 4. Conclusions

The redox process for hydrogen storage (i.e. the ability to reduce the metallic oxide and in this way be able to reproduce

hydrogen) using metallic oxides, $Fe_2O_3$, $NiFe_2O_4$ and $CuFe_2O_4$, has been proved.

The kinetic parameters for the reduction of these oxides by hydrogen have been calculated by fitting the experimental data with "*ad hoc*" models for non-catalytic gas–solid reactions.

The shrinking core + Avrami model (SCA) is shown to be a suitable model for predicting the behaviour of the reduction of $Fe_2O_3$ to Fe and the various stages involved.

The addition of second metals to form double oxides has a positive effect, since these oxides exhibit greater reaction rates.

Fundamental improvements in the redox process need to be fully understood and optimized, including the effect of several reduction–oxidation cycles on the behaviour of the solid as well as the effect of ageing on its physical properties. Once the materials have been optimized in the laboratory, practical integrated storage systems must be developed and demonstrated. At that point, design and scale-up for production and cost need to be addressed.

## Acknowledgements

The authors wish to acknowledge the financial support of DGI (Spain) for this work (REN2001-2512 and PPQ2004-01721) and the research grant AP2003-3632.

## References

[1] C.C. Elam, C.E.G. Padró, G. Sandrock, A. Luzzi, P. Lindblad, E.F. Hagen, Int. J. Hydr. Energy 28 (2003) 601.
[2] M. Momirlan, T.N. Veziroglu, Renew. Sustain. Energy Rev. 6 (2002) 141.
[3] M. Conte, P.P. Prosini, S. Passerini, Mater Sci. Eng. B 108 (2004) 2.
[4] V.P. Utigikar, T. Thiesen, Technol. Soc. 27 (2005) 315.
[5] L. Zhou, Renew. Sustain. Energy Rev. 9 (2005) 395.
[6] F. Lamani Darkrim, P. Malbrunot, G.P. Tartaglia, Int. J. Hydr. Energy 27 (2002) 193.
[7] E. David, J. Mater. Process. Technol. 162–163 (2005) 169.
[8] K. Otsuka, A. Mito, S. Takenaka, I. Yamanaka, Int. J. Hydr. Energy 26 (2001) 191.
[9] K. Otsuka, C. Yamada, T. Kaburagi, S. Takenaka, Int. J. Hydr. Energy 28 (2003) 335.
[10] K. Otsuka, T. Kaburagi, C. Yamada, S. Takenaka, J. Power Sources 122 (2003) 111.
[11] S. Takenaka, T. Kaburagi, C. Yamada, K. Nomura, K. Otsuka, J. Catal. 228 (2004) 66.
[12] S. Takenaka, N. Hanaizumi, V.T.D. Son, K. Otsuka, J. Catal. 228 (2004) 405.
[13] S. Takenaka, K. Nomura, N. Hanaizumi, K. Otsuka, Appl. Catal. A: Gen. 282 (2005) 333.
[14] K. Urasaki, N. Tanimoto, T. Hayashi, Y. Sekine, E. Kikuchi, M. Matsukata, Appl. Catal. A: Gen. 288 (2005) 143.
[15] V. Hacker, R. Frankhauser, G. Faleschini, H. Fuchs, K. Friedrich, M. Muhr, K. Kordesch, J. Power Sources 86 (2000) 531.
[16] V. Hacker, G. Faleschini, H. Fuchs, R. Fankhauser, G. Simader, M. Ghaemi, B. Spreitz, K. Friedrich, J. Power Sources 71 (1998) 226.
[17] V. Hacker, J. Power Sources 118 (2003) 311.
[18] H. Kindermann, M. Kornberger, J. Hierzer, J.O. Besenhard, V. Hacker, J. Power Sources 145 (2005) 687.
[19] V. Galvita, K. Sundmacher, Appl. Catal. A: Gen. 289 (2005) 121.
[20] P. Ciambelli, S. Cimino, G. Lasorella, L. Lisi, S. De Rossi, M. Faticanti, G. Minelli, P. Porta, Appl. Catal. B: Environ. 37 (2002) 231.
[21] M. Shimokawabe, R. Furuichi, T. Ishii, Thermochim. Acta 28 (1979) 287.
[22] F. Adam, B. Dupré, C. Gleitzer, React. Solids 7 (1989) 383.
[23] O. Levenspiel, Chemical Reactor Omnibook, Oregon State University Bookstores, 1993.
[24] J.Y. Park, O. Levenspiel, Chem. Eng. Sci. 30 (1975) 1207.
[25] J.Y. Park, O. Levenspiel, Chem. Eng. Sci. 32 (1977) 233.
[26] M. Avrami, J. Chem. Phys. 8 (1940) 212.
[27] M. Avrami, J. Chem. Phys. 9 (1941) 117.
[28] A. Faleiros, T.N. Rabelo, G.P. Thim, M.A.S. Oliveira, Mater. Res. 3 (2000) 51.
[29] H.Y. Lin, Y.W. Chen, C. Li, Thermochim. Acta 400 (2003) 61.
[30] H. Akaike, Math. Sci. 14 (1976) 5.